TEST BENCH FOR SILICON STRIP DETECTORS: FRONT-END ELECTRONICS AND DAQ

T. Petruse[1,2,*], G.L.Guardo[1,3], D.Lattuada[1,3,4], D.Choudhury[1], C.Matei[1], D.L.Balabanski[1,2], A.Oberstedt[1]

The Extreme Light Infrastructure Silicon Strip Array (ELISSA), is an experimental set-up currently under implementation at Extreme Light Infrastructure - Nuclear Physics (ELI-NP). It will be used for detailed studies of charged-particle fragments coming from key reactions in nuclear astrophysics. The set-up will consist of 36 silicon strip position sensitive detectors (PSD) assembled in a barrel-like configuration and 8 double sided silicon strip detectors (DSSSD) as end-caps.
With over 500 channels of dedicated electronics for the ELISSA experimental station, a new detector test bench has been assembled and tested for front-end electronics optimization. Using a double-sided silicon strip detector (DSSSD), various detector-electronics parameters were investigated and compared with the factory specifications of the detector. The results of these investigations - leakage currents, depletion voltage, energy resolution - are detailed in this paper.

1. Introduction

The Extreme Light Infrastructure - Nuclear Physics (ELI-NP) facility [**1**, **2**] is currently under implementation in Magurele, Romania. The Variable Energy Gamma (VEGA) System, will deliver γ-ray beams with continuous tunable gamma-ray energy over a broad energy range (from 1 to 20 MeV), small relative energy bandwidth (lower than 0.5%), high degree of linear polarization (higher than 95%), and high spectral density of 10^4 photons/(s·eV)[**3**]. Due to the unique high spectral density and small energy bandwidth of the

[1] Extreme Light Infrastructure – Nuclear Physics, Horia Hulubei National Institute for R&D in Physics and Nuclear Engineering, 30 Reactorului Str., 077125 Bucharest Magurele, Romania, e-mail: teodora.petruse@eli-np.ro

[2] Doctoral School of Engineering and Applications of Lasers and Accelerators, University Politehnica of Bucharest, 407 Atomistilor Str., IFA Building, 077125 Bucharest Magurele, Ilfov, Romania

[3] Istituto Nazionale di Fisica Nucleare - Laboratori Nazionali del Sud, Via S. Sofia, 62, 95125 Catania CT, Italia

[4] Universita degli Studi di Enna "KORE", Cittadella Universitaria - 94100 Enna (EN), Italia

VEGA system at ELI-NP, users will have the possibility to perform accurate photodisintegration reaction measurements of very low cross sections.

VEGA system implementation at ELI-NP will open the way for studies of (γ,p) and (γ,α) photodissociation reactions which are essential for stellar evolution modeling. In this type of reactions, the emitted light particles have low energies, ranging from few hundreds keV to few MeV, which requires the use of detectors capable of operating at low energy threshold. Moreover, the angular distributions should be measured over a wide angular range, leading to a better understanding of the reaction mechanism. For these type of measurements, Extreme Light Infrastructure Silicon Strip Array (ELISSA) [**4**] was proposed and it is currently under construction at ELI-NP. ELISSA will consist of three rings of twelve X3 position-sensitive detectors (PSD) [**5**] produced by Micron Semiconductor Ltd. [**6**], assembled in a barrel like configuration. The angular coverage is extended down to about 20° (160° at backward angles) by using end cap detectors such as the assembly of double sided silicon strip detectors (DSSSD). The final design is shown in Figure 1.

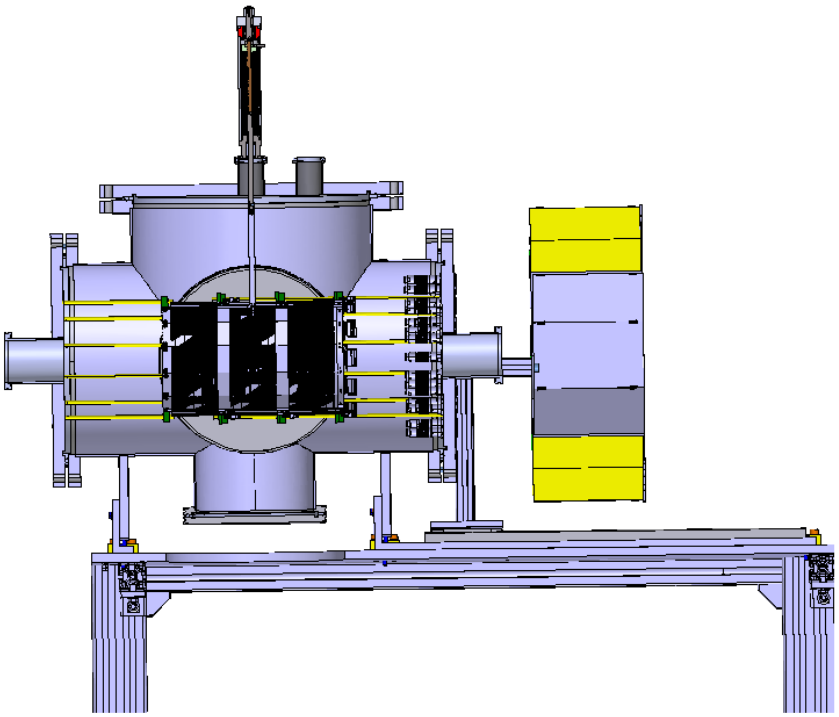

Fig. 1. Drawing of the ELISSA silicon strip detection system.

This type of array has already been successfully applied for nuclear astrophysics studies, e g. TIARA (Transfer and Inelastic All-angle Reaction Array), SHARC (Silicon Highly-segmented Array for Reactions and Coulex) or AIDA (Advanced Implantation Detector Array) [**7**, **8**, **9**].

In a recent experiment [**10**] performed at High Intensity Gamma Source (HIγS), tritons and α particles from the ^{7}Li(γ,^{3}H)^{4}He reaction were measured in coincidence using the Silicon Detector Array (SIDAR). SIDAR is made of 12 YY1 segmented silicon detectors [**11**] of different thickness and its threshold, energy and position resolution are comparable to ELISSA. The results of the ^{7}Li(γ,^{3}H)^{4}He experiment at HIγS demonstrate that silicon detectors can be used successfully to measure cross sections although beam-induced backgrounds can affect the selection of the events of interest.

The disagreement in lithium isotopes production during the Big-Bang Nucleosynthesis (BBN) is one of the unresolved question in nuclear astrophysics. There is good agreement between calculated and observed abundances for all the light nuclei except for ^{7}Li [**12**]. An accurate measurement of the ^{7}Li(γ,^{3}H)^{4}He reaction cross section down to $E_{c.m.} = 1$ MeV is also proposed as a day one experiment using ELISSA at ELI-NP. The results of the measurements with SIDAR at HIγS and GEANT4 simulations of the ELISSA detector array open the way for nuclear astrophysics experiments with the upcoming γ-ray beam at the ELI-NP facility.

In this work, a full investigation of the front-end electronics and the DAQ system of ELISSA was performed. An extensive list of parameters such as: leakage currents, depletion voltage, energy resolution was measured. The current work is motivated by the development of ELISSA detection array, as well as its optimization with respect to other existing solutions. Measurements were carried out on the Mirion [**13**] Model PF-16CT-16CD DSSSD to test the front-end electronics and performance of the DAQ system and compare the results with the data sheet of the detector.

2. **Experimental set-up**

The Mirion [**13**] Model PF-16CT-16CD DSSSD is a new detector design that consists of 16 front strips and 16 back strips, each of width 3 mm, with an interstrip distance of 0.1 mm. This provides 256 pixels of 9 mm^2 on the 25 cm^2 detector to encode x-y position of the particle hit. The thickness of the detector is 500 μm. PF-16CT-16CD DSSSD has a depletion thickness of 500 $\pm$ 25 μm and a strip capacitance of 40 pF. It has a junction window thickness smaller than 50 nm and an ohmic window thickness smaller than 1500 nm. With such a thin entrance window, the energy threshold is around 70 keV for protons and 300 keV for α-particles. The front and rear side design of the PF-16CT-16CD DSSSD is shown in Figures 2a and 2b.

A large cubical vacuum chamber was used for measurements. Inside the chamber, the detector and a standard two-peak open α-source, ^{241}Am - ^{239}Pu, were placed at a distance of 25 cm. The PF-16CT-16CD SIN 142770 detector was attached to a holder fixed to a heavy aluminum plate. All tests were carried out at a pressure between 5×10^{-6} mbar to 1×10^{-5} mbar obtained with a turbomolecular station, mounted below the vacuum chamber. Typical

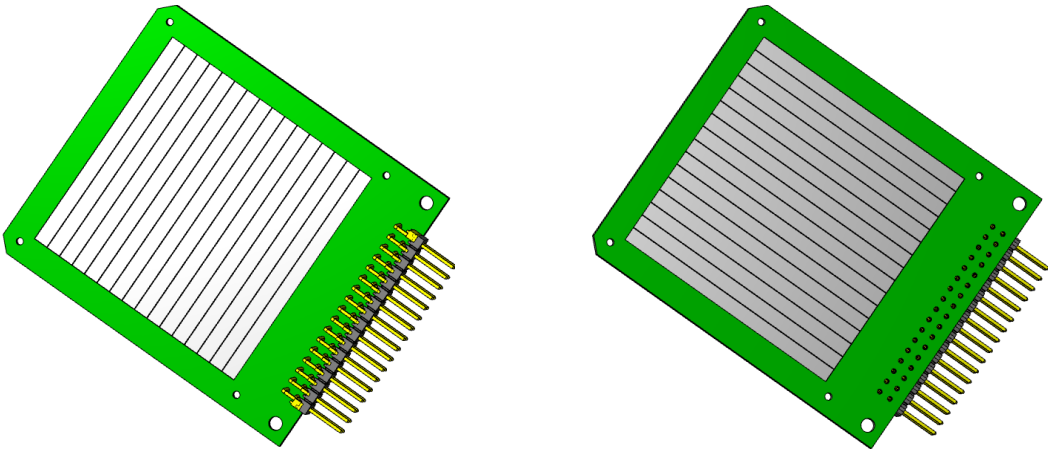

(A) Front sideof the DSSSD. (B) Rear sideof the DSSSD.

Fig. 2. The design of the PF-16CT-16CD DSSSD; it con-sists of 32 independent strips: 16 on the front side and 16 on the rear side.

energy spectra measured at the front and rear side of the PF-16CT-16CD detector are shown in Figures 3a and 3b . The measured α-spectrum in one strip is displayed with blue line. The red line represents the Gaussian fit of the α-peaks in the spectra.

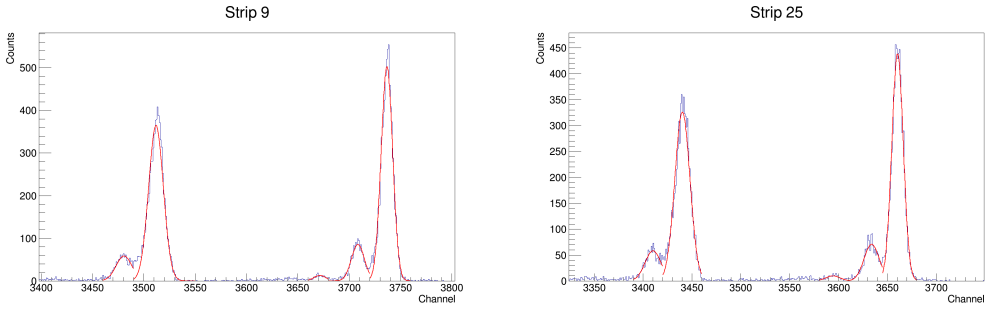

(A) Front side of the DSSSD. (B) Rear side of the DSSSD.

Fig. 3. Typical spectra measured at the front and rear side of the PF-16CT-16CD DSSSD. The blue line presents the total number of counts measured in one strip of the detector. The red lines represent the Gaussian fit of the peaks in the spectra.

Each strip was calibrated in energy by using a third order polynomial fitting procedure. The results of the fit are shown in Figure 4a for the front side of the detector and in Figure 4b for the rear side. Figures 5a and 5b represents typical energy spectra measured in one front and rear strip of the PF-16CT-16CD detector after the calibration procedure was completed. There

is a clear separation between the peaks on either the front or rear side of the DSSSD. All the values represent full width at half maximum (FWHM) value of the 5.486 MeV energy peak.

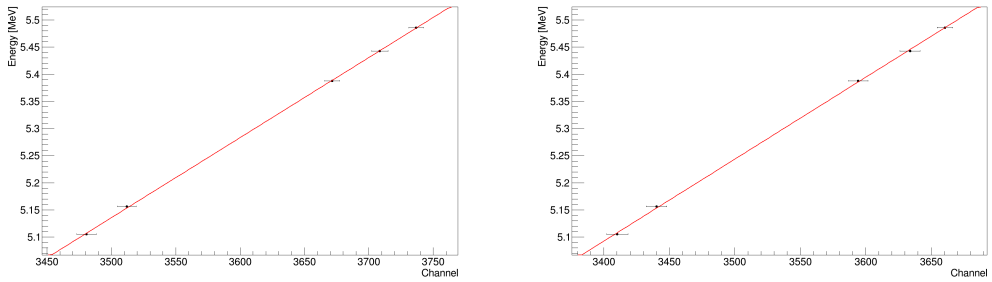

(A) Front side of the DSSSD. (B) Rear side of the DSSSD.

Fig. 4. Fitting procedure of one front and rear strip of the PF-16CT-16CD DSSSD.

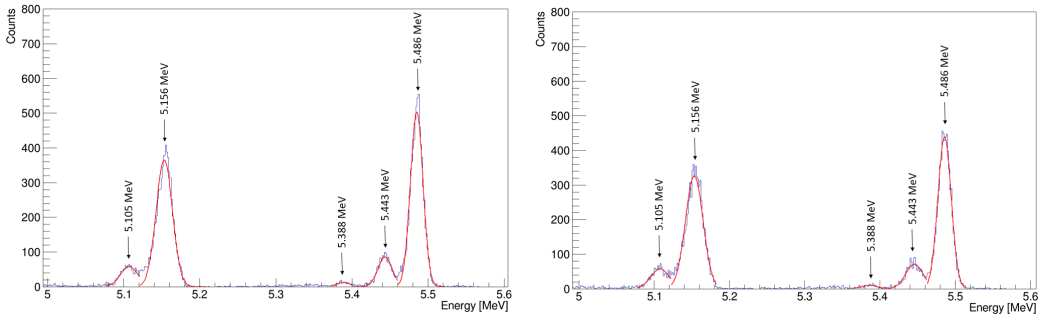

(A) Front side of the DSSSD. (B) Rear side of the DSSSD.

Fig. 5. Typical energy spectra measured at the front and rear side of the PF-16CT-16CD DSSSD using a a standard ^{241}Am - ^{239}Pu α-source. The lower-energy multiplet (with energies of 5.105 MeV and 5.156 MeV) belongs to the ^{239}Pu and the higher-energy triplet (with energies of 5.388 MeV, 5.433 MeV and 5.486 MeV) belongs to the ^{241}Am.

3. **Front-end electronics and data acquisition system**

The signal coming from PF-16CT-16CD DSSSD is processed by an electronic chain consisting of two Mesytec MPR-16 preamplifiers, two Mesytec MSCF-16 shaping / timing filter amplifiers, an Ortec [**14**] GG8020 gate generator, Mesytec 32 channel Peak Sensing ADC MADC32 and a VME controller SIS3153. The electronic chain used for the testing of PF-16CT-16CD DSSSD is shown in Fig. 6.

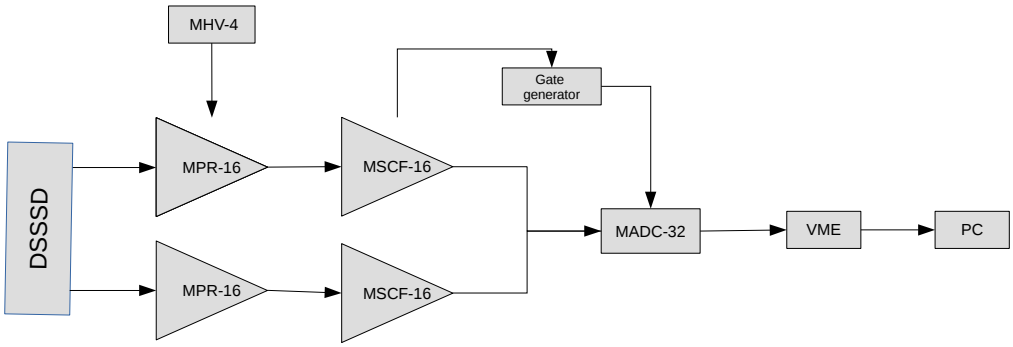

Fig. 6. The design of the electronic chain used for testing the PF-16CT-16CD DSSSD.

The MPR-16 is a state-of-the-art multichannel preamplifier module specially designed for single or double sided multi-strip silicon detectors [**15**]. In this test two MPR-16 preamplifiers were used for the 16 front and 16 back strips of a single DSSSD. The bias was given on the front side of the detector, through the MPR-16 preamplifier module. Although this module is suited for usage in vacuum, the module was used in air during the testing described in this manuscript. Using the MPR-16 preamplifier module in vacuum could in principle lower the electronic noise level. First, the chamber itself is acting like a Faraday cage, shielding the preamplifier of any external sources of noise. Another reason for achieving a lower noise level is through the shorter length of the cables as the detectors could be placed closer to the preamplifier. The MPR-16 modules were combined with two MSCF-16, shaping/timing filter amplifiers with constant fraction discriminator and multiplicity trigger and provides active baseline restorers [**15**]. These modules are well suited for multi-strip silicon detectors. The gain, threshold and different parameters were adjusted commonly in all of the strips of the DSSSD.

For acquiring the data, "mvme" VME DAQ software package was used. This is a VME DAQ by Mesytec, aimed at nuclear physics experiments. The data acquisition system it is easy to use and has basic data visualization and analysis capabilities. It allows parameter extraction, calibration, accumulation and visualization of data both during a DAQ run and while replaying from file. Additionally, a set of built-in operators can be used to perform calculations and transformations on the data as it flows through the system [**15**].

4. **Results and discussion**

The detector manufacturer provided the technical specifications which included information on the depletion voltage, bias voltage, leakage currents at 20 °C temperature, and energy resolution of the detector. The goal of the

test presented in this section is to investigate the performance of a test bench for silicon strip detectors, based on the Mesytec read-out chain and compare the results with the data sheet of the detector. The bias voltage, pole zero and shaping time were changed during the tests. This specific detector was chosen due to its large number of channels, therefore a large number of associated electronic channels.

The full depletion voltage was investigated by changing the applied voltage on the detector, from 70 V to 140 V, with a step of 10 V. Applying the bias on the front side of the detector, at low bias voltages, the rear side of the DSSSD is not fully depleted. In this situation, the rear side energy resolution is a factor of 8 worse than the front side energy resolution. In Figure 7 the energy resolution for the front side of the detector (with black) and the rear side of the detector (with red) are shown. The rear side is not fully depleted below 120 V.

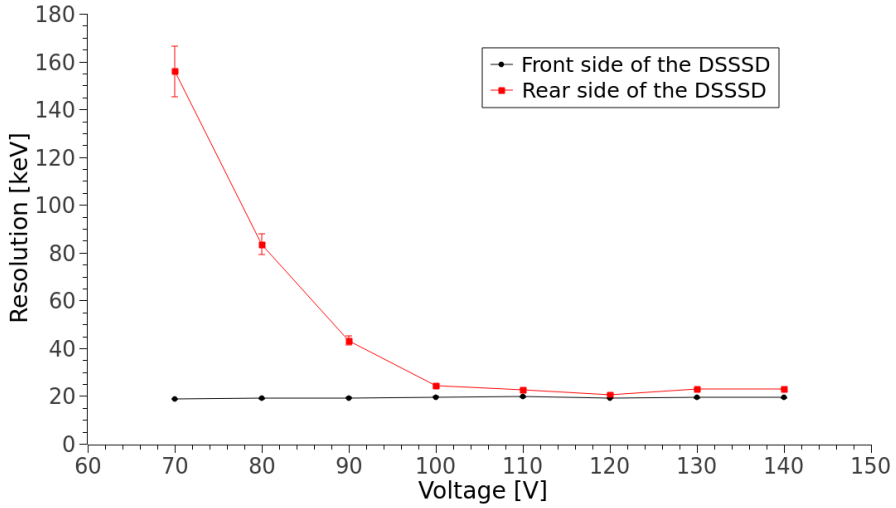

Fig. 7. Different energy resolution of the front side of the detector (with black) and the rear side of the detector (with red) based on the bias voltage.

Applying larger bias voltages on the detector, the depleted area is growing. When full depletion is achieved, the resolution is no longer influenced by the depletion area, but only by the growing leakage current. Full depletion of the DSSSD is reached at 120 V (as shown in Figure 8), which is also the recommended bias voltage by the manufacturer. For this reason, throughout the testing, the bias voltage was chosen to be 120 V.

The leakage current was monitored continuously during the measurements. During the testing, the leakage current was measured as a sum of all 16 strips of one side of the detector. Our measurements showed leakage currents of 24 ± 1 nA at 24° C. The manufacturer indicated leakage currents of 6.1

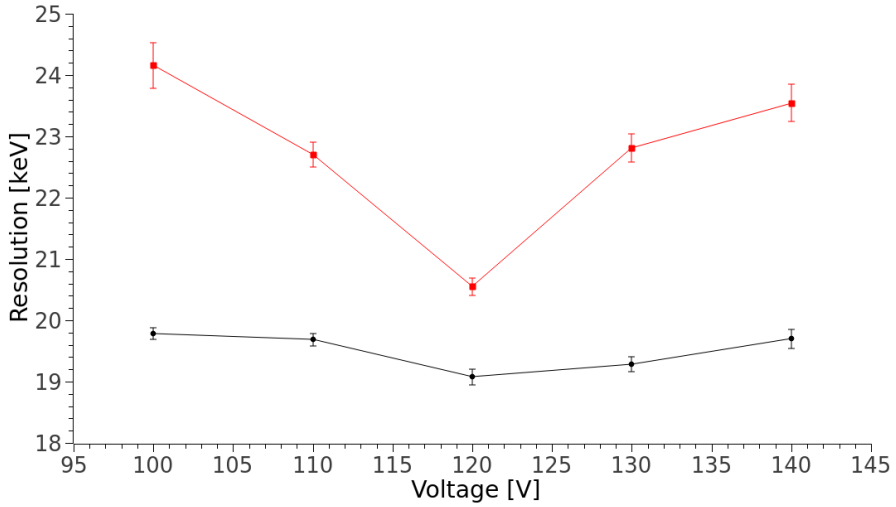

Fig. 8. Different energy resolution of the front side of the detector (with black) and the rear side of the detector (with red) based on the bias voltage.

± 2.7 nA at 20° C for each independent strip of the detector. The dependence of the leakage current on the bias voltage is shown in Figure 9.

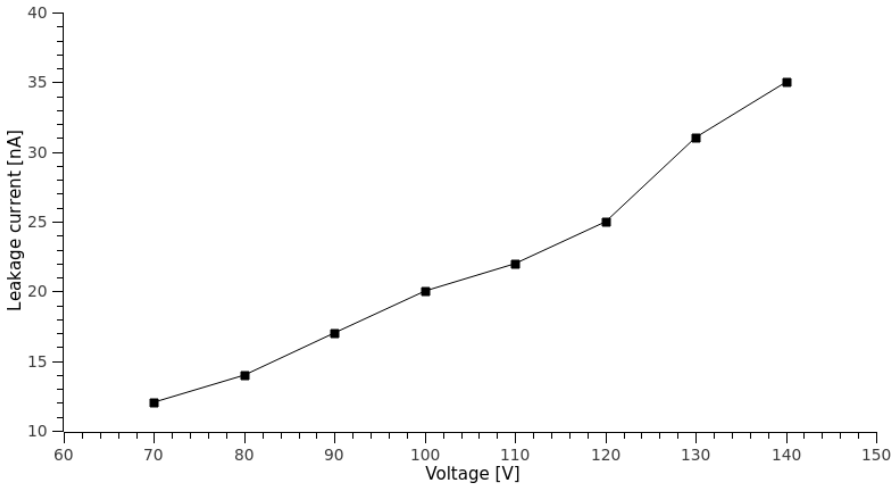

Fig. 9. Leakage current at different bias values.

The MSCF-16 shaping / timing filter amplifier is a complex module which has baseline restorers built in and it can reduce the baseline shift. When pole zero is properly adjusted, the residual baseline shift will only give a very small contribution to the energy resolution. By adjusting the pole zero, the energy resolution is improved by a factor of 1.4. The dependence of the energy resolution on pole zero on both front and rear side of the DSSSD is shown in

Figure 10. The best energy resolution is obtained with a value of the pole zero of 100 μs.

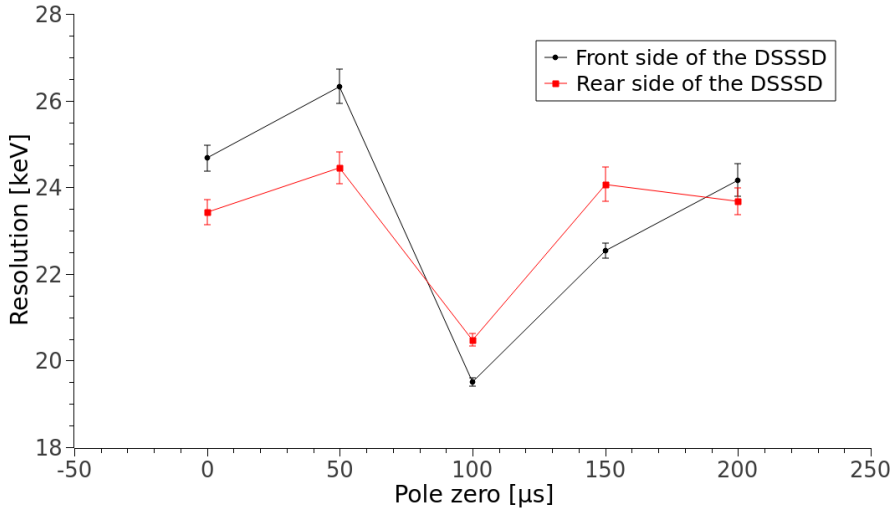

Fig. 10. The dependence of the energy resolution of the front side of the detector (with black) and the rear side of the detector (with red) on pole zero.

The dependence of the energy resolution on shaping time on both front and rear side of the DSSSD is shown in Figure 11. Changing the shaping time, the energy resolution is improved by a factor of 2.3. The best energy resolution is obtain with a value of the shaping time of 1 μs, which is also the value of the shaping time recommended by the manufacturer.

The most important characteristic of a detector is the energy resolution, reflecting its ability to separate two adjacent peaks, which allows the identification of various decays of radionuclides in the spectrum. The energy resolution obtained in all the front strips of PF-16CT-16CD detector, is in the range of 19 $\pm$ 1 keV, with a mean value of 19.2 keV. The rear side of the detector showed an energy resolution in the range of 20.5 $\pm$ 1 keV, with a mean value of 20.4 keV. Moreover, in Figures 12a and 12b it is shown that there is a difference of approximately 1 keV in resolution between the front and the rear side of the DSSSDs. These values are slightly better than the energy resolution reported by the manufacturer, which is 24.5 $\pm$ 3.5 keV. The slight difference in the mean energy resolution obtained during this testing and the energy resolution given by the manufacturer might come from the small leakage current reached during the testing.

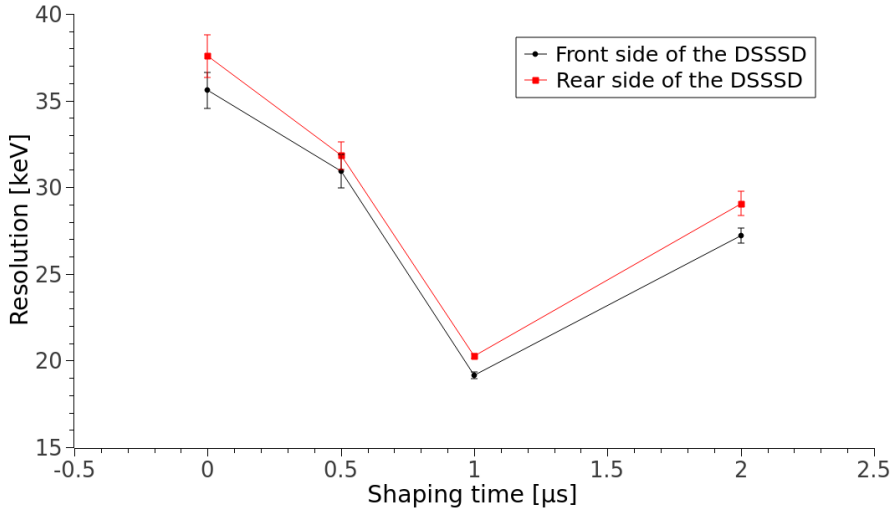

Fig. 11. Dependence of the energy resolution of the front side of the detector (with black) and the rear side of the detector (with red) on shaping time.

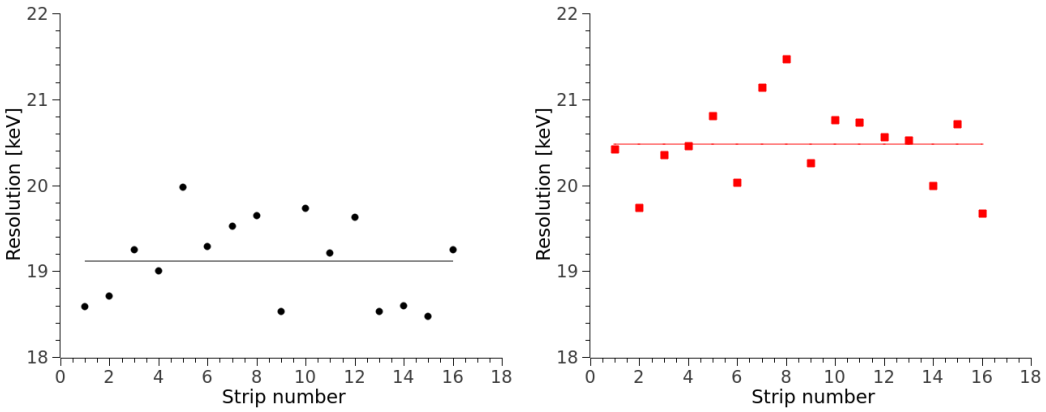

(A) Front side of the DSSSD. (B) Rear side of the DSSSD.

Fig. 12. The dependence of the energy resolution of the front side of the detector (with black) and the rear side of the detector (with red) on the strip number. The straight line represents the mean value of the energy resolution on the front side (with black) and the rear side (with red) of the detector.

5. Conclusions

A new silicon strip detector test bench including front-end electronics and DAQ was implemented at ELI-NP. Mirion DSSSD model PF-16CT-16CD was tested for the first time outside the laboratories of the producer. Measurement of the energy resolution on the front and rear side showed excellent results,

with a energy resolution below 22 keV on both sides. These values are slightly better than the energy resolution reported by the manufacturer, which is 24.5 $\pm$ 3.5 keV. The slight difference in the mean energy resolution obtained during this testing and the energy resolution given by the manufacturer might come from the smaller leakage current reached during this testing. The leakage current was around 25 nA. The read-out chain consisted of two Mesytec MPR-16 preamplifiers, two Mesytec MSCF-16 is a shaping/timing filter amplifiers, a GG8020 gate generator, Mesytec 32 channel Peak Sensing ADC MADC32 and an USB VME controller SIS3153. The "mvme" DAQ provides an easy to use data acquisition system with data visualization, allowing on-line and of-line basic analysis of the data.

Acknowledgments

This work is supported by the Extreme Light Infrastructure Nuclear Physics Phase II, a project co-financed by the Romanian Government and the European Union through the European Regional Development Fund - the Competitiveness Operational Programme (1/07.07.2016, COP, ID1334).

REFERENCES

[1] N. V. Zamfir, *Extreme Light Infrastructure - Nuclear Physics (ELI-NP)*, 2015, Nucl. Phys. News, 25(3), 34.

[2] S. Gales, K. A. Tanaka, D. L. Balabanski, F. Negoita, D. Stutman, O. Tesileanu, C. A. Ur, D. Ursescu, I. Andrei, S. Ataman, M. O. Cernaianu, L. D'Alessi, I. Dancus, B. Diaconescu, N. Djourelov, D. Filipescu, P. Ghenuche, D. G. Ghita, C. Matei, K. Seto, M. Zeng, N. V. Zamfir, *The extreme light infrastructure—nuclear physics (ELI-NP) facility: new horizons in physics with 10 PW ultra-intense lasers and 20 MeV brilliant gamma beams*, 2018, Rep. Prog. Phys., 81, 9, 094301.

[3] VEGA System Technical Design Report, to be published.

[4] O. Tesileanu, M. Gai, A. Anzalone, C. Balan, J. Bihalowicz, M. Cwiok, W. Dominik, S. Gales, D. G. Ghita, Z. Janas, D. Kendellen, M. La Cognata, C. Matei, K. Mikszuta-Michalik, C. Petcu, M. Pfützner, T. Matulewicz, C. Mazzocchi, C. Spitaleri, *Charged particle detection at ELI-NP*, 2016, Rom. Rep. Phys., 68, 699-734.

[5] S. Chesnevskaya, D.L. Balabanski, D. Choudhury, P. Constantin, D.M. Filipescu, D.G. Ghita, G.L. Guardo, D. Lattuada, C. Matei, A. Rotaru, A. State, *Performance studies of X3 silicon detectors for the future ELISSA array at ELI-NP*, 2018, J. Instrum., 13, 05, T05006.

[6] Micron Semiconductor, General catalogue, http://www.micronsemiconductor.co.uk.

[7] Labiche, M. and Catford, W.N. and Lemmon, R.C. and Timis, C.N. and Chapman, R. and Orr, N.A. and Fernández-Domínguez, B. and Moores, G. and Achouri, N.L. and Amzal, N. and et al., *TIARA: A large solid angle silicon array for direct reaction studies with radioactive beams*, 2010, Nucl. Instrum. Meth. Phys. Res. A, 614, 439–448.

[8] Diget, C and Fox, S and Smith, A and Williams, Scott and Porter-Peden, M and Achouri, L and Adsley, P and Falou, Hicham and Austin, R. and Ball, G and Blackmon, J and Brown, S and Catford, W and Chen, A and Chen, Jun and Churchman, R and Dech, J. and Valentino, D and Djongolov, M and Wilson, Gemma, *SHARC:*

Silicon Highly-segmented Array for Reactions and Coulex used in conjunction with the TIGRESS g-ray spectrometer, 2011, J. Instrum., 02, P02005.

[9] C. J. Griffin, T. Davinson, A. Estrade, D. Braga, I. Burrows, P. J. Coleman-Smith, T. Grahn, A. Grant, L. J. Harkness-Brennan, G. Kiss, M. Kogimtzis, I. H. Lazarus, S. C. Letts, Z. Liu, G. Lorusso, K. Matsui, S. Nishimura, R. D. Page, M. Prydderch, V. H. Phong, V. F. E Pucknell, S. Rinta-Antila, O. J. Roberts, D. A. Seddon, J. Simpson, S. L. Thomas, P. J. Woods, *β-Decay Studies of r-Process Nuclei Using the Advanced Implantation Detector Array (AIDA)*, 2017, JPS Conf. Proc. 14, 020622.

[10] M. Munch, C. Matei, S. D. Pain, M. T. Febbraro, K. A. Chipps, H. J. Karwowski, C. Aa. Diget, A. Pappalardo, S. Chesnevskaya, G. L. Guardo, D. Walter, D. L. Balabanski, F. D. Becchetti, C. R. Brune, K. Y. Chae, J. Frost-Schenk, M. J. Kim, M. S. Kwag, M. La Cognata, D. Lattuada, R. G. Pizzone, G. G. Rapisarda, G. V. Turturica, C. A. Ur, Y. Xu, *Measurement of the* $^{7}\mathrm{Li}(\gamma,t)^{4}\mathrm{He}$ *ground-state cross section between* $E_\gamma = 4.4$ *and 10 MeV*, 2020, Phys. Rev. C, 101, 055801.

[11] K. A. Chipps, D. W. Bardayan, K.Y. Chae, J. A. Cizewski, R. L. Kozub, C. Matei, B. H. Moazen, C. D. Nesaraja, P. D. O'Malley, S. D. Pain, W. A. Peters, S. T. Pittman, K. T. Schmitt, M. S. Smith, *^{28}Si(p,^{3}He) reaction for spectroscopy of ^{26}Al*, 2012, Phys. Rev. C 86, 014329.

[12] B.D. Fields, *The Primordial Lithium Problem*, 2011, Annu. Rev. Nucl. Part. Sci. 61, 47.

[13] Mirion, General catalogue, http://www.mirion.com.

[14] Ortec, General catalogue, https://www.ortec-online.com.

[15] Mesytec, General catalogue, http://www.mesytec.com.